Biochemistry

 Volume 39, Number 35 September 5, 2000

Accelerated Publications

Interaction between Two Discontiguous Chain Segments from the β-Sheet of *Escherichia coli* Thioredoxin Suggests an Initiation Site for Folding†

María Luisa Tasayco,*,‡ James Fuchs,§ Xiao-Min Yang,‡ Donita Dyalram,‡ and Roxana E. Georgescu‡

Biochemistry Division, Department of Chemistry, The City College of New York, 138th Street and Convent Avenue, New York, New York 10031, and Department of Biochemistry, Molecular Biology and Biophysics, University of Minnesota, 1479 Gortner Avenue, St. Paul, Minnesota 55108

Received April 4, 2000; Revised Manuscript Received June 1, 2000

ABSTRACT: The approach of comparing folding and folding/binding processes is exquisitely poised to narrow down the regions of the sequence that drive protein folding. We have dissected the small single α/β domain of oxidized *Escherichia coli* thioredoxin (Trx) into three complementary fragments (N, residues 1−37; M, residues 38−73; and C, residues 74−108) to study them in isolation and upon recombination by far-UV CD and NMR spectroscopy. The isolated fragments show a minimum of ellipticity of ca. 197 nm in their far-UV CD spectra without concentration dependence, chemical shifts of H_α that are close to the random coil values, and no medium- and long-range NOE connectivities in their three-dimensional NMR spectra. These fragments behave as disordered monomers. Only the far-UV CD spectra of binary or ternary mixtures that contain N- and C-fragments are different from the sum of their individual spectra, which is indicative of folding and/or binding of these fragments. Indeed, the cross-peaks corresponding to the rather hydrophobic β_2 and β_4 regions of the β-sheet of Trx disappear from the $^1H-^{15}N$ HSQC spectra of isolated labeled N- and C-fragments, respectively, upon addition of the unlabeled complementary fragments. The disappearing cross-peaks indicate interactions between the β_2 and β_4 regions, and their reappearance at lower temperatures indicates unfolding and/or dissociation of heteromers that are predominantly held by hydrophobic forces. Our results argue that the folding of Trx begins by zippering two discontiguous and rather hydrophobic chain segments (β_2 and β_4) corresponding to neighboring strands of the native β-sheet.

Although biophysicists still debate whether the burst phase intermediates observed in the folding of small proteins truly represent folding events (*1*−*4*), the current emphasis is on determining the balance between the local and nonlocal interactions that drives the folding of small proteins. An interesting idea that is gaining ground is that the folding events are primarily determined by the overall topology of the final fold and not by specific details of the stabilizing interactions (*5*, *6*). If this is the case, the wealth of information about protein evolution arising from structural genomics promises significant insights into the protein folding problem and its possible solution by integrating theory and experiments (*6*) in the study of representative protein domains.

† Financial aid was provided by the RCMI grant from the NIH to CCNY, NIH Grant GM53808, and NSF Grant MCB-9507255 to M.L.T., who is an NSF CAREER Awardee.

* To whom correspondence should be addressed. E-mail: mltj@mafalda.sci.ccny.cuny.edu. Phone: (212) 650-8169. Fax: (212) 795-4301.

‡ The City College of New York.

§ University of Minnesota.

10.1021/bi000761e CCC: $19.00
Published on Web 08/11/2000

Folding processes that bring together discontiguous and disordered chain segments without the assistance of interconnecting regions show that nonlocal interactions can be responsible for driving folding. Such processes are found in small homodimers [GCN4 (*7*) and ArcR (*8*)] and in artificially generated heterodimers [CI2 (*9*), barnase (*10*), and Trx[1] (*11*−*13*)] that resemble their native structures. In principle, the regions that are involved in these nonlocal interactions can be found by further dissecting the protein and studying folding and/or binding of the resulting fragments. For instance, mixing experiments with cytochrome *c* (Cyt *c*) fragments corresponding to the N- and C-terminal chain segments indicate the formation of a rather helical noncovalent complex in the presence of covalently linked heme (*14*) and exogenous heme (*15*). The formation of this complex correlates well with folding events in which amide groups become protected only in chain segments corresponding to the N- and C-terminal helices (*16*). As another example, fragment complementation studies of the α-helical homodimer tryptophan repressor (TrpR) indicate that dimerization of its N-terminal fragment precedes the complementation and reassembly of the full structure (*17*). Subsequent kinetic studies of the native-like homodimer of a similar N-terminal fragment of TrpR (*18*) shed light on the complex folding kinetics of the full protein. These studies illustrate the usefulness of comparing folding and folding/binding (*19*−*21*) processes to gather structural insight about the folding of α-helical proteins.

To extend this approach to α/*β* proteins, we have studied the folding of oxidized *Escherichia coli* thioredoxin (Trx) (*22*) and the folding/binding of its complementary fragments (*23*). The kinetic model of folding for this five-stranded *β*-sheet packed against four α-helices (see Figure 1a) shows multiple pathways going through burst phase intermediates of hydrophobic nature, rich in *β*-type structures, which reflect both Pro-independent and -dependent processes. To narrow down the regions of its polypeptide sequence that are responsible for reassembly upon cleavage of a loop (*13*, *24*) or a helix (*11*), three complementary fragments (N, residues 1−37; M, residues 38−73; and C, residues 74−108) were generated. Here we report the results of studying the isolated and recombined fragments by size exclusion chromatography and far-UV CD and $^1H-^{15}N$ NMR spectroscopy. Our studies suggest that the folding of Trx begins by zippering two discontiguous and rather hydrophobic chain segments corresponding to two neighboring strands of the native *β*-sheet.

MATERIALS AND METHODS

E. coli Trx, its fragments, and their ^{15}N-labeled versions were prepared according to previous reports (*11*, *23*). The lyophilized isolated fragments were resuspended in 4 or 6 M GuHCl and 10 mM phosphate buffer (KP_i) (pH 7.0) and dialyzed against KP_i (pH 6.5) for NMR spectroscopy or against KP_i (pH 7.0) for CD spectroscopy. The fragments were mixed before and after dialysis for NMR and CD spectroscopy, respectively. Serial dilutions of freshly prepared solutions were carried out to monitor the concentration dependence of the isolated fragments. The molar extinction

[1] Abbreviations: CD, circular dichroism; NMR, nuclear magnetic resonance; Trx, thioredoxin.

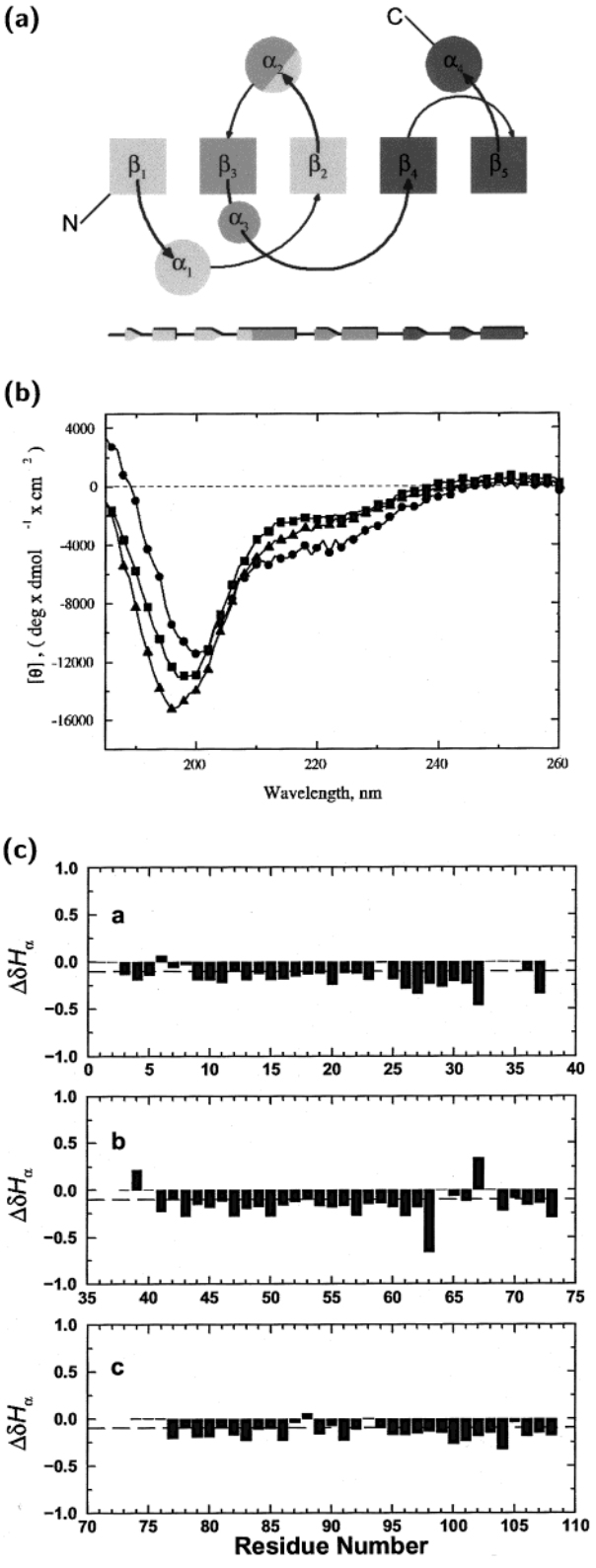

FIGURE 1: (a) Topological scheme of Trx (*32*) depicting the N-fragment (light gray), the M-fragment (gray), and the C-fragment (dark gray). Helices and strands are depicted as circles and boxes, respectively. The smallest circle corresponds to the distorted α_3 helix (*33*). The elements of secondary structure are also depicted along the primary sequence. (b) Far-UV CD spectra of the N-fragment (●), the M-fragment (▲), and the C-fragment (■). (c) Plot of the observed chemical shift values for the H_α protons of an isolated fragment minus that of the random coil: the N-fragment (a), the M-fragment (b), and the C-fragment (c).

coefficients of the N- and M-fragments in KP_i are 1.12×10^4 and 2.56×10^3 M^{-1} cm^{-1} at 280 nm (*25*), respectively, and that of the C-fragment is 3.96×104 M^{-1} cm^{-1} at 214 nm (*23*). Size exclusion chromatography was carried out with a peptide column from Pharmacia using a Pharmacia FPLC system and 10 mM KP_i (pH 7.0).

Far-UV CD Spectroscopy. Spectra were obtained with an AVIV-60DS instrument using cells with a path length of 1 or 0.1 mm. The spectra represent the average of four scans at 20° after correction for the buffer baseline.

NMR Spectroscopy. NMR data were acquired on a 500 MHz Varian Unity plus spectrometer at various temperatures. Two-dimensional $^1H-^{15}N$ HSQC spectra were recorded using 16 scans under the phase-sensitive mode with 100 and 768 complex in t_1 and t_2, respectively. The spectral widths were 7600.2 Hz in the ^1H dimension and 2200 Hz in the ^{15}N dimension. Three-dimensional TOCSY-HSQC and three-dimensional NOESY-HSQC spectra were acquired using 16 scans, three spectral widths ($\omega_1 = 5999.7$ Hz, $\omega_2 = 1555.7$ Hz, and $\omega_3 = 6800.4$ Hz), and mixing times of 70 and 200 ms, respectively. All spectra were processed and analyzed on a Silicon Graphics computer using Felix 1.10 and 2.3 (Biosym Technologies, San Diego, CA). Three-dimensional TOCSY-HSQC and three-dimensional NOESY-HSQC spectra were used to identify through-bond and through-space connectivities for each fragment. The assignment of the TOCSY-HSQC spectra began with residues such as Gly, Thr, and Ala. All glycines with the exception of G33 were assigned on the basis of the $NH-H_\alpha$ cross-peaks. The alanines were characterized by their $NH-H_\alpha$ and $NH-\beta CH_3$ cross-peaks in the TOCSY. Threonines and valines were assigned on the basis of $NH-H_\alpha$, $NH-H_\beta$, and $NH-\gamma CH_3$ cross-peaks in the TOCSY spectrum. The AMX spin systems were identified by the H_β chemical shifts in the TOCSY spectrum. Those residues with long side chains such as Lys, Leu, and Ile were assigned on the basis of NOE connectivities. The NOESY and TOCSY spectra were used to obtain sequential connectivities [$d(H_{\alpha i}, NH_{i+1})$, $d(H_{\beta i}, NH_{i+1})$, and $d(NH_i, NH_{i+1})$] according to standard procedures.

RESULTS AND DISCUSSION

Isolated Fragments Are Disordered. Freshly prepared solutions of the isolated N-, M-, and C-fragments (Figure 1a), under conditions that promote their monomeric state (*23*), elute from a size exclusion chromatography column at 10.85, 10.27, and 10.48 mL, respectively. The far-UV CD spectra of freshly prepared solutions of the isolated N-, M-, and C-fragments at neutral pH exhibited no concentration dependence within the experimental range (5−375 μM), a minimum between 197 and 200 nm, and a bulge between 210 and 230 nm, which is more pronounced in the case of the N-fragment (see Figure 1b). The unexpectedly higher elution volume, the shifted minimum, and the pronounced bulge in the far-UV CD spectrum of the N-fragment suggest the presence of residual structure in this fragment. The one-dimensional NMR spectra of these fragments at pH 6.5 exhibit a narrow chemical shift dispersion for the amide protons of ca. 0.8 ppm, and no upfield peaks between 0 and −1 ppm. Only the N-fragment shows both a 30% decrease of the signal-to-noise ratio in the one-dimensional NMR spectrum and partial elution in the void volume of the size exclusion chromatography column after incubation for 3 days at room temperature, which is indicative of a slow oligomerization. Despite the fact that the N-fragment appears to have a residual structure that promotes slow oligomerization, all these isolated fragments behave as disordered monomers.

To further search for residual structure in these fragments, three-dimensional NMR experiments were carried out. The N-fragment, which oligomerized slowly, produced resonances whose half-width show no concentration dependence (*11*), which suggests the coexistence of monomers and oligomers with high molecular weights. Most residues, with the exception of Pro (positions 34, 40, 64, 68, and 76) and a few others (positions 1, 2, 33, 38, 74, and 75), were assigned. Some amide protons share the same chemical shift values such as those at positions 16 and 36, 19 and 22, 25 and 27, 80 and 102, 81 and 98, 84 and 97, 85 and 104, 86 and 100, and 95 and 106. The H_αs of these fragments show chemical shifts that are close to the random coil values and dispersions of <0.3 ppm (Figure 1c). Further analysis of the spectra of these fragments shows the typical network of $d(H_{\alpha i}, NH_{i+1})$ and $d(H_{\beta i}, NH_{i+1})$ connectivities. Although a few connectivities between protons from residues separated by two peptide bonds were found, no evidence for medium- or long-range interactions was observed (data not shown). In summary, the far-UV CD and NMR spectra of monomeric N-, M-, and C-fragments show no evidence of a well-defined conformational bias.

N- and C-Fragments Interact with Each Other. On the basis of our previous success reassembling Trx by recombination of two complementary fragments (residues 1−73 and 74−108 or 1−37 and 38−108) (*11*−*13*, *24*), we proceeded to narrow down the regions of the sequence responsible for recognition and reassembly by searching for pairs of smaller fragments (residues 1−37, 38−73, and 74−108) that interact with each other. Three techniques, which together cover a wide range of concentrations (size exclusion chromatography and far-UV CD and NMR spectroscopy), were used to detect both tight and weak complexes. No evidence for the presence of new species different from any of the isolated fragments was observed when injecting binary mixtures at millimolar concentrations into a size exclusion chromatography column. Since we suspected that the lack of evidence for interactions was due to the dilution effect of the chromatography column, far-UV CD measurements were carried out with the isolated and recombined fragments using a final concentration range of 5−375 μM (see Figure 2). To start with, three binary mixtures (N/M, M/C, and N/C) were prepared, each containing the first fragment (100 μM) and the second one (375 μM) to keep a constant fragment ratio. It is interesting to observe that the difference in the spectra of the N/M and M/C mixtures are negligible compared with that of the N/C mixture. In fact, further addition of the C-fragment to the N/M mixture or of the N-fragment to the M/C mixture until reaching a final concentration of 100 μM demonstrates that an excess of the M-fragment has less effect than an excess of the C-fragment on the difference spectra of the original binary mixtures. Furthermore, addition of the M-fragment to the N/C mixture up to a final concentration of 100 μM produces negligible change in the original difference spectrum. It should be mentioned that, qualitatively, all the difference spectra exhibit a predominance of β-type structures.

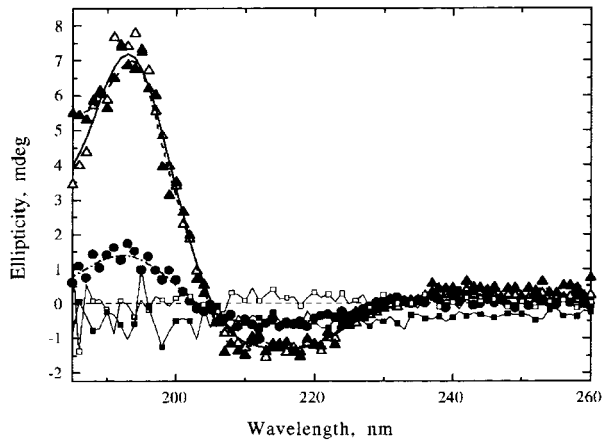

FIGURE 2: Difference far-UV CD spectra between binary or ternary mixtures and their corresponding isolated fragments: the N-fragment (100 μM) and the M-fragment (375 μM) depicted with black squares, the M-fragment (100 μM) and the C-fragment (375 μM) depicted with white squares, the N-fragment (100 μM) and the C-fragment (375 μM) depicted with black triangles, the N-fragment (100 μM), the M-fragment (100 μM), and the C-fragment (375 μM) depicted in white triangles, and the N-fragment (100 μM), the M-fragment (375 μM), and the C-fragment (100 μM) in white circles. The buffer was KP_i at pH 7.0 and 20 °C in all cases.

The next step was to test whether the same phenomenon is observed at millimolar concentrations using NMR spectroscopy. The $^1H-^{15}N$ HSQC spectra of mixtures containing a single labeled fragment (0.7 or 0.8 mM) and the unlabeled complementary fragment (1.4 or 1.6 mM) were compared with those of the corresponding isolated labeled fragment at the same concentration (Figure 3a). The spectra of mixtures of the labeled M- with the unlabeled N- or C-fragment show no evidence of interaction. However, the spectra of the binary mixture of N- and C-fragments at a ratio of 1:2 or 2:1 exhibit fewer cross-peaks than those of the corresponding isolated fragment. In fact, this effect is further enhanced upon addition of the M-fragment to the binary mixture until reaching a final concentration of 0.7 or 0.8 mM.

These mixing experiments demonstrate that the N- and C-fragments interact primarily with each other to form heteromers which appear rich in β-type structures and whose interactions with the M-fragment are negligible under these experimental conditions.

Disappearance of Cross-Peaks Points to the Importance of β_2 and β_4. The absence of cross-peaks for certain residues in the NMR spectrum of a given protein can be due to the combination of the slow overall tumbling of a large structure with the rapid movement of disordered tails (*26*, *27*) or to conformational fluctuations of a moderately sized structure at an intermediate time scale (*28*). Thus, the presence of fewer cross-peaks in the HSQC spectra of the N/C mixtures and the fading of some of them might reflect the formation of heteromers with different degrees of oligomerization. Inspection of the $^1H-^{15}N$ HSQC spectra (Figure 3a) indicates that, despite the overlapping resonances and the absence of cross-peaks for P76, essentially every cross-peak of the spectra corresponding to regions of β_2 (A22, I23, L24, V25, D26, F27, W28, and A29) and β_4 (P76, T77, L78, L79, L80, F81, and K82) in the native state disappears from the spectra of the isolated labeled N- and C-fragments, respectively, upon addition of the unlabeled complementary fragments. These spectra also indicate the complete or almost complete disappearance of cross-peaks corresponding to residues in the regions of β_1 (4), α_1 (16 and 17), α_2 (35−37), β_5 (89, 90, and 92), α_4 (96−100, 102, and 104−106), and the interconnecting segments (3, 18, 19, 21, 30−32, 83, 84, 86, 87, and 95). We should stress that, regardless of whether the heteromers of the N- and C-fragments are large or small, the vanishing cross-peaks are not randomly located. The fact that they include residues not only from the regions of β_2 and β_4 but also from others which are close in the native structure (α_1, α_2, β_5, α_4, and interconnecting segments; see Figure 1a) argue in favor of native-like interactions between N- and C-fragments. An interesting observation is that the disappearing peaks only occur when the mixture contains these fragments. This is somewhat surprising, since inspection of the native structure shows that the isolated C-fragment and the binary mixture of the N- and M-fragments also have the possibility of forming native-like contacts (see Figure 1a), but no supporting NMR evidence was found in those cases. This behavior strongly suggest that native-like interactions between β_2 and β_4 are more stable than the other possibilities. We interpret our NMR results by postulating that zippering of two rather hydrophobic regions, corresponding to β_2 and β_4 in the native state, constitutes the first operational folding and/or binding event between the N- and C-fragments.

Nature of the Hypothetical Interaction between β_2 and β_4. To establish the nature of the interactions within the hypothetical N/C complex and to explore whether slowing the conformational exchange produces new cross-peaks (*29*), the HSQC spectra of the isolated and recombined fragments were acquired within a temperature range from 3 to 46 °C. When the ternary mixture containing the labeled N-fragment is cooled from 20 to 3 °C, the HSQC spectra show the reappearance of cross-peaks for all amide protons with the exception of those for the C-terminal end of the extended β_2 and the imidazole protons of Trp28 and -31 (Figure 3a). This tendency is even more noticeable in the spectrum of the binary mixture of the N-fragment and the labeled C-fragment, where every cross-peak reappears upon cooling from 20 to 5 °C (Figure 3a). This reappearance is consistent with an increase in the population of the isolated fragments due to unfolding and/or dissociation of heteromers. The temperature dependence of the difference far-UV CD spectra of the binary and ternary mixtures of fragments shows a similar trend, although their persistence at 5 °C indicates an incomplete unfolding and/or dissociation process. This behavior is typical of processes driven by the hydrophobic effect (*30*, *31*) and correlates well with the hydrophobic nature of the interacting β_2 and β_4 regions.

Initiation Site of the Folding of Trx. Our far-UV CD and NMR results strongly suggest that the disordered monomeric N- and C-fragments undergo some kind of native-like hydrophobic interactions through the β_2 and β_4 regions. We are aware, however, that the disordered nature of the isolated fragments does not preclude the existence of flickering local interactions that might promote recognition between β_2 and β_4. The fact that the interactions seem to involve mainly the hydrophobic regions of the β-sheet in the native state correlates well with the observation of hydrophobic β-rich burst phase intermediates in the folding of Trx (*22*). We therefore put forth the following provocative hypothesis: the

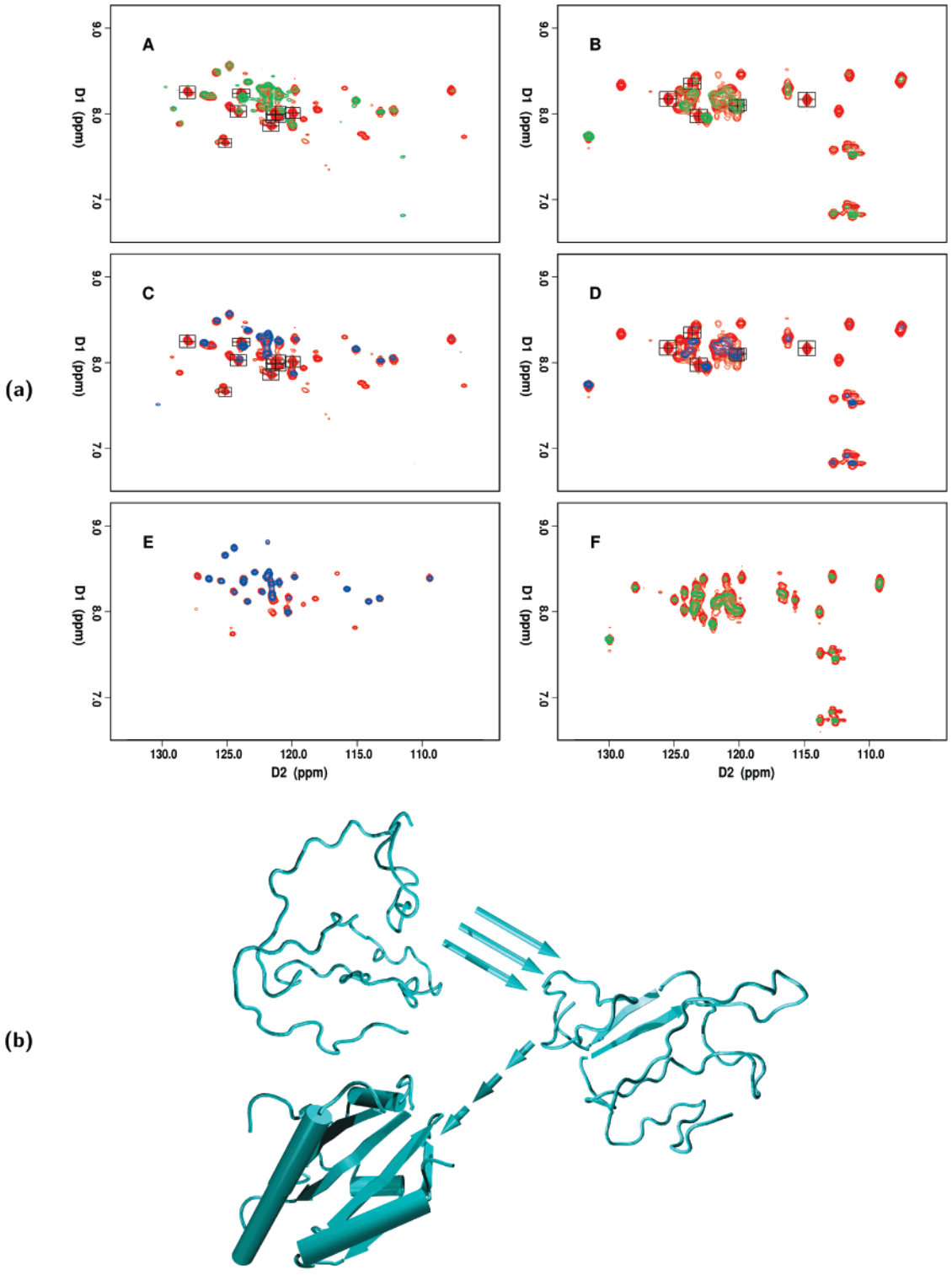

FIGURE 3: (a) HSQC spectra of isolated ^{15}N-labeled fragments and that of their binary and ternary mixtures with unlabeled fragments (six panels). Cross-peaks for the segments corresponding to β_2 and β_4 of Trx are boxed in black. (A) Spectrum of the mixture of the labeled N-fragment (0.8 mM) with the unlabeled C-fragment (1.6 mM) in 0.1 mM KP_i at pH 6.5 (green) overlayed on that of the isolated ^{15}N-labeled N-fragment (0.8 mM) in 0.1 mM KP_i at pH 6.5 (red) at 20 °C. (B) Spectrum of the mixture of the unlabeled N-fragment (1.6 mM) and the labeled C-fragment (0.8 mM) in 0.1 mM KP_i at pH 6.5 (green) overlayed on that of the isolated ^{15}N-labeled C-fragment (0.8 mM) in 0.1 mM KP_i at pH 6.5 (red) at 20 °C. (C) Spectrum of the ternary mixture of the labeled N-fragment (0.7 mM), the M-fragment (0.7 mM), and the C-fragment (1.4 mM) in KP_i at pH 6.5 (blue) overlayed on that of the isolated ^{15}N-labeled N-fragment (0.8 mM) in 0.1 mM KP_i at pH 6.5 (red) at 20 °C. (D) Spectrum of the ternary mixture of the N-fragment (1.4 mM), the M-fragment (0.7 mM), and the labeled C-fragment (0.7 mM) in KP_i at pH 6.5 (blue) overlayed on that of the isolated ^{15}N-labeled C-fragment (0.8 mM) in 0.1 mM KP_i at pH 6.5 (red) at 20 °C. (E) Spectrum of the ternary mixture of the labeled N-fragment (0.7 mM), the M-fragment (0.7 mM), and the C-fragment (1.4 mM) in KP_i at pH 6.5 (blue) overlayed on that of the isolated ^{15}N-labeled N-fragment (0.8 mM) in 0.1 mM KP_i at pH 6.5 (red) at 3 °C. (F) Spectrum of the binary mixture of the N-fragment (1.6 mM) and the labeled C-fragment (0.8 mM) in 0.1 mM KP_i at pH 6.5 (green) overlayed on that of the isolated ^{15}N-labeled C-fragment (0.8 mM) in 0.1 mM KP_i at pH 6.5 (red) at 5 °C. (b) Cartoon depicting the folding of Trx by zippering of the hydrophobic and discontiguous chain segments corresponding to β_2 and β_4. The cartoon was generated with the program VMD (*34*).

zippering of two discontiguous and rather hydrophobic chain segments, corresponding to β_2 and β_4 in the native β-sheet, serves to initiate the folding of Trx-like proteins (see Figure 3b).

ACKNOWLEDGMENT

We thank Francisco Figueirido for helpful discussions. The use of the NMR facilities of Hunter College is gratefully acknowledged.

SUPPORTING INFORMATION AVAILABLE

NOE connectivities of the isolated fragments. This material is available free of charge via the Internet at http://pubs.acs.org.

REFERENCES

1. Jennings, P. A. (1998) *Nat. Struct. Biol. 5*, 846−848.
2. Jackson, S. E. (1998) *Folding Des. 3*, R81−R91.
3. Qi, P.-X., Sosnick, T. R., and Englander, S. W. (1998) *Nat. Struct. Biol. 5*, 882−884.
4. Roder, H., and Shastry, M. C. R. (1999) *Curr. Opin. Struct. Biol. 9*, 620−626.
5. Goldenberg, D. P. (1999) *Nat. Struct. Biol. 6*, 987−990.
6. Alm, E., and Baker, D. (1999) *Curr. Opin. Struct. Biol. 9*, 189−196.
7. Zitzewitz, J. A., Bilsel, O., Luo, J., Jones, B. E., and Matthews, C. R. (1995) *Biochemistry 34*, 12812−12819.
8. Milla, M. E., and Sauer, R. T. (1994) *Biochemistry 33*, 1125−1133.
9. Neira, J. L., Davis, B., Ladurner, A. G., Buckle, A. M., dePrat Gay, G., and Fersht, A. R. (1996) *Folding Des. 1*, 189−208.
10. Sancho, J., and Fersht, A. R. (1992) *J. Mol. Biol. 224*, 741−747.
11. Yang, X.-M., Yu, W.-F., Li, J.-H., Fuchs, J., Rizo, J., and Tasayco, M. L. (1998) *J. Am. Chem. Soc. 120*, 7985−7986.
12. Yang, X.-M., Georgescu, R., Li, J.-H., Yu, W., Haierhan, and Tasayco, M. L. (1999) Recognition between disordered polypeptide chains from cleavage of an α/β domain: Self- versus non-self-association, In *Proceedings of the 1999 Pacific Symposium on Biocomputing*, Vol. 4, pp 590−600.
13. Yu, W.-F., Tung, C.-S., Wang, H., and Tasayco, M. L. (2000) *Protein Sci. 9*, 20−28.
14. Wu, L. C., Laub, P. B., Elöve, G. A., Carey, J., and Roder, H. (1993) *Biochemistry 32*, 10271−10276.
15. Kang, X., and Carey, J. (1999) *J. Mol. Biol. 289*, 463−468.
16. Roder, H., Elöve, G. A., and Englander, S. W. (1988) *Nature 335*, 700−704.
17. Tasayco, M. L., and Carey, J. (1992) *Science 255*, 594−597.
18. Gloss, L. M., and Matthews, C. R. (1998) *Biochemistry 37*, 15990−15999.
19. Taniuchi, H., Parr, G. R., and Jullierat, M. A. (1986) *Methods Enzymol. 131*, 185−217.
20. dePrat Gay, G. (1996) *Protein Eng. 9*, 843−847.
21. Tsai, C.-J., Xu, D., and Nussinov, R. (1998) *Folding Des. 3*, 71−80.
22. Georgescu, R., Li, J.-H., Goldberg, M., Tasayco, M. L., and Chaffotte, A. (1998) *Biochemistry 37*, 10286−10297.
23. Chaffotte, A., Li, J.-H., Goldberg, M., and Tasayco, M. L. (1997) *Biochemistry 36*, 16040−16048.
24. Tasayco, M. L., and Chao, K. (1995) *Proteins: Struct., Funct., Genet. 22*, 41−44.
25. Mulvey, R. S., Gualtieri, R. J., and Beychok, S. (1974) *Biochemistry 13*, 782.
26. Landry, S. J., Zeilstra-Ryalls, Fayet, O., Georgopoulos, C., and Gierasch, L. M. (1993) *Nature 364*, 255−258.
27. Fiebig, K. M., Rice, L. M., Pollock, E., and Brunger, A. T. (1999) *Nat. Struct. Biol. 6*, 117−123.
28. Schulman, B. A., Kim, P. S., Dobson, C. M., and Redfield, C. (1997) *Nat. Struct. Biol. 4*, 630−634.
29. Barbar, E. (1999) *Biopolymers 51*, 191−207.
30. Baldwin, R. L. (1986) *Proc. Natl. Acad. Sci. U.S.A. 83*, 8069−8072.
31. Makhatadze, G. I., and Privalov, P. L. (1995) *Adv. Protein Chem. 47*, 307−425.
32. Dyson, H. J., Holmgren, A., and Wright, P. E. (1989) *Biochemistry 28*, 7074−7087.
33. Jeng, M. F., Campbell, A. P., Begley, T., Holmgren, A., Wright, P. E., and Dyson, H. J. (1994) *Structure 2*, 853.
34. Humphrey, W., Dalke, A., and Schulten, K. (1996) *J. Mol. Graphics 14*, 33−38.

BI000761E